10032 *Inorg. Chem.* **2010**, *49*, 10032–10040
DOI: 10.1021/ic1013363

Inorganic Chemistry
Article

Preparation, Properties, and Crystal Structures of Organometallic Ionic Liquids Comprising 1-Ferrocenyl-3-alkylimidazolium-Based Salts of Bis(trifluoromethanesulfonyl)amide and Hexafluorophosphate

Yuji Miura,[†] Fumiko Shimizu,[†,‡] and Tomoyuki Mochida*[,†]

[†]*Department of Chemistry, Graduate School of Science, Kobe University, Rokkodai, Nada, Hyogo 657-8501, Japan, and* [‡]*Department of Chemistry, Faculty of Science, Toho University, Miyama, Funabashi, Chiba 274-8510, Japan*

Received July 5, 2010

Bis(trifluoromethanesulfonyl)amide (TFSA), hexafluorophosphate (PF_6^-), and iodide salts of 1-ferrocenyl-3-alkylimidazolium were prepared and their thermal and physical properties, including the dependence on alkyl chain length (methyl−hexadecyl), were investigated. The TFSA salts were highly viscous ionic liquids with melting points around room temperature. 1-Ferrocenyl-4-methyltriazolium salts were also prepared for comparison. The ferrocenylimidazolium and ferrocenyltriazolium cations showed redox waves for both the ferrocenyl moiety and the azolium moiety and exhibited corresponding charge-transfer bands at around 330 nm, which were analyzed using the Marcus−Hush model. Crystal structure determinations at low temperature revealed that the PF_6 and iodide salts form layerlike structures composed of ionic layers of the charged moieties. The TFSA salt exhibited short hydrogen-bond-like intermolecular contacts between the hydrogen atoms of the cation and oxygen atoms of the anion.

Introduction

Ionic liquids (ILs) have recently attracted special attention from the viewpoint of physical and materials chemistry,[1−6] and their properties have been investigated in terms of their application as reaction solvents and electrolytes for electrochemical devices.[7−15] Onium cations are generally used as components of ILs, and in particular, alkylimidazolium salts form the broadest family. One of the methods for incorporating additional functionality into ILs is to add functional moieties, such as organometallic substituents, to their constituents.[16−22] For this purpose, we recently prepared ferrocenium ILs that contain ferrocenium cations.[23] In addition, we have prepared a series of ferrocene-based heterocyclic ligands and their coordination compounds.[24−28] Ferrocene can act as an electron donor exhibiting a redox function,[29]

*To whom correspondence should be addressed. E-mail: tmochida@platinum.kobe-u.ac.jp.

(1) Stark, A.; Seddon, K. R. In *Kirk−Othmer Encyclopedia of Chemical Technology*, 5th ed.; Wiley-Interscience: New York, 2007; Vol. *26*, pp 836−919.
(2) *Ionic Liquids: Industrial Applications to Green Chemistry*; Rogers, R. D., Seddon, K. R., Eds.; ACS Symposium Series; American Chemical Society: Washington, D.C., 2002; Vol. *818*.
(3) Armand, M.; Endres, F.; MacFarlane, D. R.; Ohno, H.; Scrosati, B. *Nat. Mater.* **2009**, *8*, 621–629.
(4) Krossing, I.; Slattery, J. M.; Daguenet, C.; Dyson, P. J.; Oleinikova, A.; Weingärtner, H. *J. Am. Chem. Soc.* **2006**, *128*, 13427–13434.
(5) Weingärtner, H. *Angew. Chem., Int. Ed.* **2008**, *47*, 654–670.
(6) Yoshida, Y.; Saito, G. *Phys. Chem. Chem. Phys.* **2010**, *12*, 1675–1684.
(7) Plechkova, N. V.; Seddon, K. R. *Chem. Soc. Rev.* **2008**, *37*, 123–150.
(8) *Ionic Liquids in Synthesis*; Wasserscheid, P., Welton, T., Eds.; Wiley-VCH: Weinheim, Germany, 2003.
(9) Welton, T. *Chem. Rev.* **1999**, *99*, 2071–2083.
(10) Dupont, J.; de Souza, R. F.; Suarez, P. A. Z. *Chem. Rev.* **2002**, *102*, 3667–3692.
(11) Lancaster, N. L.; Salter, P. A.; Welton, T.; Young, G. B. *J. Org. Chem.* **2002**, *67*, 8855–8861.
(12) Wasserceid, P.; Keim, W. *Angew. Chem., Int. Ed.* **2000**, *39*, 3772–3789.
(13) Song, C. E.; Roh, E. J. *Chem. Commun.* **2000**, 837–838.
(14) *Electrochemical Aspects of Ionic Liquids*; Ohno, H., Ed.; John Wiley and Sons: New York, 2005.
(15) Matsumoto, H.; Sakaebe, H.; Tatsumi, K.; Kikuta, M.; Ishiko, E.; Kono, M. *J. Power Sources* **2006**, *160*, 1308–1313.
(16) Wang, W.; Balasubramanian, R.; Murray, R. W. *J. Phys. Chem. C* **2008**, *112*, 18207–18216.
(17) Gao, Y.; Twamley, B.; Shreeve, J. M. *Inorg. Chem.* **2004**, *43*, 3406–3412.
(18) Matsumoto, H. JP Patent 277 393, 2003.
(19) Lee, C. K.; Hsu, K. -M.; Tsai, C. -H.; Lai, C. K.; Lin, I. J. B. *Dalton Trans.* **2004**, 1120–1126.
(20) Iida, M.; Baba, C.; Inoue, M.; Yoshida, H.; Taguchi, E.; Furusho, H. *Chem.—Eur. J.* **2008**, *14*, 5047–5056.
(21) Lee, S. -g. *Chem. Commun.* **2006**, 1049–1063.
(22) Cole, A. C.; Jensen, J. L.; Ntai, I.; Tran, K. L. T.; Weaver, K. J.; Forbes, D. C.; Davis, J. H., Jr. *J. Am. Chem. Soc.* **2002**, *124*, 5962–5963.
(23) Inagaki, T.; Mochida, T. *Chem. Lett.* **2010**, *39*, 572–573.
(24) Mochida, T.; Shimizu, F.; Shimizu, H.; Okazawa, K.; Sato, F.; Kuwahara, D. *J. Organomet. Chem.* **2007**, *692*, 1834–1844.
(25) Horikoshi, R.; Mochida, T.; Moriyama, H. *Inorg. Chem.* **2002**, *41*, 3017–3024.
(26) Mochida, T.; Okazawa, K.; Horikoshi, R. *Dalton Trans.* **2006**, 693–704.
(27) Horikoshi, R.; Nambu, C.; Mochida, T. *Inorg. Chem.* **2003**, *42*, 6868–6875.
(28) Horikoshi, R.; Ueda, M.; Mochida, T. *New J. Chem.* **2003**, *27*, 933–937.
(29) *Ferrocenes: Homogeneous Catalysis, Organic Synthesis, Materials Science*; Togni, A., Hayashi, T., Eds.; VCH: Weinheim, Germany, 1995.

Published on Web 10/06/2010

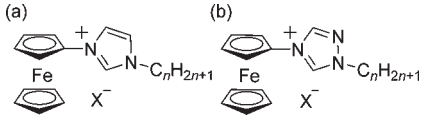

Figure 1. Chemical formulas of (a) 1-ferrocenyl-3-alkylimidazolium salts and (b) 1-ferrocenyl-4-methyltriazolium salts.

from which donor−acceptor molecules can be prepared by introducing electron accepting moieties.[30] Ferrocene-based donor−acceptor-type molecules have attracted attention because of their photochemical properties, such as photoinduced electron transfer,[31−33] and optical properties, such as third-order harmonic generation.[34−37]

To date, several ILs containing ferrocenyl substituents have been reported,[16−18,38,39] but the cations in these compounds contain bridging groups between the ferrocenyl moiety and the cationic group, such as methylene or ester units. In this study, we prepared a series of 1-ferrocenyl-3-alkylimidazolium salts with varying alkyl chain lengths [n = 1 (**1**), 2 (**2**), 3 (**3**), 4 (**4**), 6 (**5**), 8 (**6**), 12 (**7**), and 16 (**8**)] (Figure 1a) in which the ferrocenyl group is directly conjugated to the electron-accepting imidazolium moiety. Electronic features such as redox activities and photoinduced electron transfer are added to the ILs with incorporation of the conjugated ferrocenyl moiety. Furthermore, it is of interest to understand how the introduction of the nonplanar and bulky ferrocenyl substituent affects the melting points and phase sequences of the salts. As the counteranions, we chose bis(trifluoromethanesulfonyl)amide (abbreviated as TFSA), which provided ILs at room temperature, and hexafluorophosphate (PF_6^-), which provided crystalline solids. Thermal properties, viscosities, redox potentials, and charge-transfer (CT) absorption bands for these salts were investigated and analyzed. As a reference compound, 1-ferrocenyl-4-methyltriazolium salt [n=1 (**9**); Figure 1b] was prepared. To investigate structural aspects, some of these salts were characterized crystallographically at low temperature.

Results and Discussion

Preparation and Properties. 1-Ferrocenyl-3-alkylimidazolium iodides [**1**][I]−[**8**][I] were prepared by reacting *N*-ferrocenylimidazole with the corresponding iodoalkanes. These iodide salts were liquids except for the methyl and ethyl derivatives, and were generally unstable with respect to light, probably due to photodecomposition.[40]

Table 1. Intramolecular Charge-Transfer Absorption Maxima, $E_T(30)$ Values, and the Corresponding Dimensionless E_T^N Values

compd	λ_{max} (nm)	$E_T(30)$ (kcal mol^{-1})	E_T^N
[**1**][TFSA]	550	52.0	0.657
[**2**][TFSA]	570	50.2	0.601
[**4**][TFSA]	578	49.5	0.579
[**6**][TFSA]	582	49.1	0.569

TFSA salts were obtained by metathesis of the iodide salts and LiTFSA in water, with the TFSA salts separating from the water layer as red-brown liquids. The yields for [**1**][TFSA]−[**8**][TFSA] (99−35%) decreased with increasing alkyl chain length because separation from the water phase became less efficient. The TFSA salts were obtained as liquids, but it was found by DSC measurements (vide infra) that they are in a supercooled state at room temperature. [**5**][TFSA]−[**7**][TFSA] did not crystallize at low temperature, while the other liquids could be crystallized by repeatedly applying external stimuli at low temperatures. A single crystal of [**4**][TFSA], which was grown by careful recrystallization, was subjected to X-ray structure analysis (vide infra). [**1**][PF_6]−[**8**][PF_6] were also prepared by metathesis and were obtained as yellow crystalline solids. The TFSA and PF_6 salts were soluble in polar organic solvents and insoluble in water and nonpolar organic solvents. Although these salts were sufficiently stable, decomposition occurred gradually when the salts were dissolved in dimethyl sulfoxide or exposed to UV light.

E_T^N values for the TFSA salts were estimated using the absorption maximum (λ_{max}) of the lowest-energy band of the Reichardt's dye 2,6-diphenyl-4-(2,4,6-triphenyl-*N*-pyridino)phenolate when dissolved in these liquids.[41,42] E_T^N correlates with the acceptor number (AN) of the solvents, ranging from 1 (water) to 0 (TMS). The determined E_T^N values are listed in Table 1 and range from 0.657 for [**1**][TFSA] to 0.569 for [**6**][TFSA]. These values are comparable to those of alcohols and typical imidazolium-based ILs (E_T^N = 0.5−0.7).[41−43] The polarity decreased with increasing alkyl chain length, which is probably due to the increase in the size of the nonpolar moieties. A similar tendency has been reported for 1-alkyl-3-methylimidazolium salts with TFSA ([$C_n$mim][TFSA]), in which the E_T^N values ranged from 0.670 for C_1mim to 0.630 for C_8mim.[44] The smaller values for the present salts are probably ascribable to the strong electron releasing ferrocenyl substituent, which decreases the charge density on the imidazolium cation, thereby reducing the acceptor ability of the solvent.

Melting Points and Glass-Transition Temperatures. Melting points (T_m) and glass-transition temperatures (T_g) of the TFSA and PF_6 salts determined by DSC analysis are summarized in Table 2. In most of the salts, no crystallization occurred in the cooling run (10 K min^{-1}) from the liquid state and only glass transitions were observed, while [**8**]-[TFSA], [**1**][PF_6], [**7**][PF_6], and [**8**][PF_6] crystallized with a thermal hysteresis of 30−50 K.

The T_m of the TFSA salts ranged from 34.6 °C for [**1**][TFSA] to 50.1 °C for [**4**][TFSA], as plotted in Figure 2,

(30) Mochida, T.; Yamazaki, S. *J. Chem. Soc., Dalton Trans.* **2002**, 3559–3564.
(31) Conti, F.; Corvaja, C.; Gattazzo, C.; Toffoletti, A.; Bergo, P.; Maggini, M.; Scorrano, G.; Prato, M. *Phys. Chem. Chem. Phys.* **2001**, *3*, 3526–3531.
(32) Rovira, C.; Ruiz-Molina, D.; Elsner, O.; Vidal-Gancedo, J.; Bonvoisin, J.; Launay, J. -P.; Veciana, J. *Chem.—Eur. J.* **2001**, *7*, 240–250.
(33) Lloveras, V.; Caballero, A.; Tárraga, A.; Velasco, M. D.; Espinosa, A.; Wurst, K.; Ebans, D. J.; Vidal-Gancedo, J.; Rovira, C.; Molina, P.; Veciana, J. *Eur. J. Inorg. Chem.* **2005**, 2436–2450.
(34) Long, N. J. *Metallocenes: An Introduction to Sandwich Complexes*; Blackwell Science: Oxford, U.K., 1998; chapter 6, and references cited therein.
(35) Green, M. L. H.; Marder, S. R.; Thompson, M. E.; Bandy, J. A.; Bloor, D.; Kolinsky, P. V.; Jones, R. J. *Nature* **1987**, *330*, 360–362.
(36) Barlow, S.; Bunting, H. E.; Ringham, C.; Green, J. C.; Bublitz, G. U.; Boxer, S. G.; Perry, J. W.; Marder, S. R. *J. Am. Chem. Soc.* **1999**, *121*, 3715–3723.
(37) Nalwa, H. S. *Mater. Lett.* **1997**, *33*, 23–26.
(38) Thomas, J. -L.; Howarth, J.; Hanlon, K.; McGuirk, D. *Tetrahedron Lett.* **2000**, *41*, 413–416.
(39) Nyamori, V. O.; Gumede, M.; Bala, M. D. *J. Organomet. Chem.* **2010**, *695*, 1126–1132.
(40) Utepova, I. A.; Chupakhin, O. N.; Charushin, V. N. *Heterocycles* **2008**, *76*, 39–72.
(41) Weingärtner, H. *Z. Phys. Chem.* **2006**, *220*, 1395–1405.
(42) Reichardt, C. *Green Chem.* **2005**, *7*, 339–351.
(43) Fletcher, K. A.; Storey, I. A.; Hendricks, A. E.; Pandey, S.; Pandey, S. *Green Chem.* **2001**, *3*, 210–215.
(44) Tokuda, H.; Tsuzuki, S.; Susan, M. A. B. H.; Hayamizu, K.; Watanabe, M. *J. Phys. Chem. B* **2006**, *110*, 19593–19600.

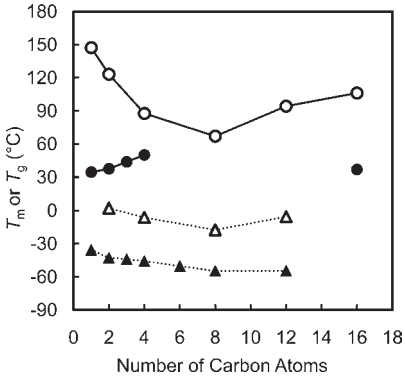

Figure 2. Melting points (T_m) and glass-transition temperatures (T_g) of 1-ferrocenyl-3-alkylimidazolium salts plotted against alkyl chain lengths. Plots include T_m (●) and T_g (▲) of TFSA salts, and T_m (○) and T_g (△) of PF_6 salts.

Table 2. Melting Points (T_m), Glass-Transition Temperatures (T_g), and Relevant Thermodynamic Parameters of the TFSA and PF_6 salts of **1**−**8**

compd	T_m (°C)	ΔH (kJ mol^{-1})	ΔS (J mol^{-1} K^{-1})	T_g (°C)	T_g/T_m
[**1**][TFSA]	34.6	15.6	50.4	−35.5	0.772
[**2**][TFSA]	37.6	12.6	40.2	−42.7	0.742
[**3**][TFSA]	43.9	13.6	42.8	−44.0	0.723
[**4**][TFSA]	50.1	30.6	94.4	−45.7	0.704
[**5**][TFSA]				−50.4	
[**6**][TFSA]				−54.7	
[**7**][TFSA]				−54.5	
[**8**][TFSA]	40.0	52.6	166.4		
[**1**][PF_6]	147.2	24.2	57.3		
[**2**][PF_6]	123.2	24.4	61.3	2.2	0.695
[**4**][PF_6]	87.7	18.5	50.8	−6.2	0.740
[**6**][PF_6]	67.0	22.2	64.7	−17.5	0.752
[**7**][PF_6]	94.2	34.6	93.7	−5.5	0.729
[**8**][PF_6]	106.2	41.3	108.5		

and are higher by ca. 13−54 K than those of the corresponding [$C_n$mim][TFSA].[45,46] This difference is attributed to the increased molecular volume and weight of the ferrocenyl group. In contrast with [$C_n$mim][TFSA],[47] the melting points of the TFSA salts increased with increasing alkyl chain length, which is probably due to the apparent increase of symmetry with respect to the imidazolium ring. Additionally, the melting points may be affected by the packing efficiency, which is possibly correlated with alkyl chain length. For example, the matching of the size of the TFSA anion and the butyl substituent in [**4**][TFSA] seemed to afford closer packing in the crystal (vide infra). Conversely, the glass transition temperatures decreased with increasing alkyl chain length similar to the case of [$C_n$mim][TFSA].[47] The different dependence of T_g and T_m on alkyl chain length is a characteristic feature of these salts. In the PF_6 salts, however, T_g and T_m exhibited the same trend. With increasing alkyl chain length, T_m decreased for C_1−C_8 from 147 °C ([**1**][PF_6]) to 67 °C ([**6**][PF_6]) and subsequently increased, and T_g followed the same trend. This tendency resembles that of [$C_n$mim][PF_6],[48] but the decrease of T_m for C_1−C_8 is only about one-third of that observed for

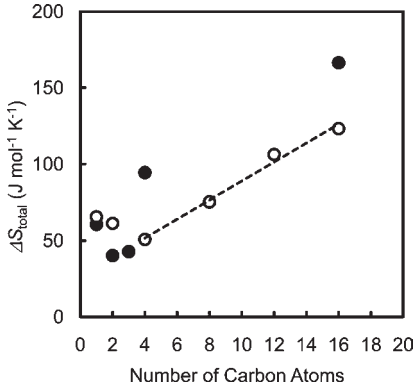

Figure 3. Dependence of the total entropies of [**1**][TFSA]−[**8**][TFSA] (●) and [**1**][PF_6]−[**8**][PF_6] (○) on alkyl-chain length.

Table 3. Data for Crystalline Phase Transitions

compd	crystalline phase	T (°C)	ΔH (kJ mol^{-1})	ΔS (J mol^{-1}K^{-1})
[**1**][TFSA]	II → I	−25.9	2.5	10.2
[**8**][TFSA]	II[a] → I	12.8	−9.5	−33.0
[**1**][PF_6]	II → I	119.9	3.3	8.3
[**6**][PF_6]	II → I	−26.5	26.7	10.6
[**7**][PF_6]	II → I	16.2	3.7	12.6
[**8**][PF_6]	III → II	38.4	2.4	7.6
	II → I	58.2	3.2	9.3
	I → IV	40.9	4.6	14.8
	IV → I	34.4	4.4	14.0

[a] Metastable phase.

[$C_n$mim][PF_6], resulting in a much higher T_m. An empirical relationship $T_g/T_m = 2/3$ is known to hold generally for molecular compounds[49,50] including [$C_n$mim][TFSA] and [$C_n$mim][PF_6].[46,51] In the present salts, deviation from this relationship became larger for TFSA salts with shorter chains and PF_6 salts with longer chains (Table 2). The T_m and T_g of [**1**][TFSA] are lower than those of [1-(ferrocenylmethyl)-3-methylimidazolium][TFSA] (T_g = −32.2 °C) and [(ferrocenylmethyl)trimethylammonium][TFSA] (T_m = 89 °C) by ca. 50−55 °C,[17] whereas the T_m of [**1**][PF_6] (147 °C) is much higher than that of [1-(ferrocenylmethyl)-3-methylimidazole][PF_6] (T_m = 66−68 °C).[39]

The alkyl-chain-length dependence of the total entropies of the TFSA and PF_6 salts is shown in Figure 3. Total entropy was defined as the sum of the transition entropies as the salts changed from the stable phase to liquids. With increasing alkyl chain length (C_4−C_{16}), the entropies of the PF_6 salts increased by 6.2 J mol^{-1} K^{-1} per one methylene group, and the same trend seemed to hold for the TFSA salts based on the comparison of [**4**][TFSA] and [**8**][TFSA]. These values are smaller than the entropy changes found for [$C_n$mim][TFSA], which increased by 9.3 J mol^{-1} K^{-1} per one methylene group.[52,53] This

(45) Bonhôte, P.; Dias, A. -P.; Papageorgiou, N.; Kalyanasundaram, K.; Grätzel, M. *Inorg. Chem.* **1996**, *35*, 1168–1178.
(46) Dzyuba, S. V.; Bartsch, R. A. *ChemPhysChem.* **2002**, *3*, 161–166.
(47) Holbrey, J. D.; Reichert, W. M.; Rogers, R. D. *Dalton Trans.* **2004**, 2267–2271.
(48) López-Martin, I.; Burello, E.; Davey, P. N.; Seddon, K. R.; Rothenberg, G. *ChemPhysChem.* **2007**, *8*, 690–695.
(49) Turnbull, D.; Cohen, M. H. *Modern Aspect of the Vitreous State*; Butterworth: London, 1960; Vol. *1*, p 38.
(50) Yamamuro, O.; Minamimoto, Y.; Inamura, Y.; Hayashi, S.; Hamaguchi, H. *Chem. Phys. Lett.* **2006**, *423*, 371–375.
(51) Tokuda, H.; Hayamizu, K.; Ishii, K.; Susan, M. A. B. H.; Watanabe, M. *J. Phys. Chem. B* **2004**, *108*, 16593–16600.
(52) Shimizu, Y.; Ohte, Y.; Yamamura, Y.; Saito, K. *Chem. Phys. lett.* **2009**, *470*, 295–299.
(53) Paulechka, Y. U.; Blokhin, A. V.; Kabo, G. J.; Strechan, A. A. *J. Chem. Thermodyn.* **2007**, *39*, 866–877.

Table 4. Viscosities, Activation Energies, and Parameters of the VFT Equations for the TFSA Salts

compd	η at 25 °C (mPa s)	E_a (kJ mol^{-1})	T_0 (°C)	η_0 (Pa s)	η_g (MPa s)	D
[**1**][TFSA]	3499	91.9	−63.1	4.80×10^{-4}	979	3.72
[**2**][TFSA]	1267	77.2	−84.0	1.21×10^{-4}	4.86	5.34
[**5**][TFSA]	1163	59.1	−118.2	2.31×10^{-5}	0.193	10.00
[**6**][TFSA]	1382	67.1	−129.7	5.01×10^{-6}	0.831	13.53
[C_4mim][TFSA][a]	49	31.3	−108.5			4.65
[butyferrocenium][TFSA][b]	112	38.8	−106.8	3.33×10^{-4}		4.61

[a] See ref 56. [b] See ref 57.

difference is probably due to the larger molecular volumes of the ferrocenyl salts, for which thermal contributions from the alkyl group are less important.

Phase transitions were observed in the solid state in [**1**][TFSA], [**8**][TFSA], [**1**][PF_6], and [**6**][PF_6]−[**8**][PF_6], whereas no other salts exhibited phase transitions down to −180 °C. Table 3 shows the data for the crystalline phase transitions in each salt. Most salts exhibited two crystalline phases, denoted as I and II, where II is the low-temperature phase. In [**8**][TFSA], a metastable phase was observed. On cooling at 2 K min^{-1}, crystallization of the liquid occurred at −7.0 °C to form a metastable phase (phase II), and heating of this phase led to an exothermic transition to phase I, followed by melting at 40.0 °C. Crystals of phase I was obtained by recrystallization. In [**8**][PF_6], there were three stable crystalline phases (I, II, III) and a metastable phase (IV). A schematic Gibbs free energy diagram for [**8**][PF_6] is shown in Figure S1 in the Supporting Information. Cooling from the liquid state produced a solid (phase III) due to supercooling, and upon heating this phase transformed to phase II, then phase I, and then melted. Cooling of phase I led to the metastable phase IV due to supercooling (DSC traces are shown in Figure S2 in the Supporting Information). Although some imidazolium salts exhibit plastic phases[54] and liquid crystal phases,[55] such phases were not observed in the present salts.

Viscosities. Viscosities of the TFSA salts at 25 °C for [**1**][TFSA], [**2**][TFSA], [**5**][TFSA], and [**6**][TFSA] were 3499, 1267, 1163, and 1382 mPa s, respectively (Table 4). The compounds were confirmed to be Newtonian fluids. These liquids were much more viscous than alkylimidazolium (e.g., 49 mPa s for [C_4mim][TFSA][56]) and ferrocenium ILs (e.g., 112 mPa s for [butylferrocenium][TFSA][23]), and [**1**][TFSA] in particular was highly viscous. The temperature dependence of the viscosities is shown in Figure S3 in the Supporting Information. The activation energies (E_a) determined from an Arrhenius approximation ranged from 91.9 kJ mol^{-1} for [**1**][TFSA] to 59.1 kJ mol^{-1} for [**5**][TFSA] (Table 4). These values are two to three times larger than those of alkylimidazolium[56] and ferrocenium[57] salts (E_a = 30−40 kJ mol^{-1}), and E_a became smaller with increasing alkyl chain length. The temperature dependence was further analyzed based on a Vogel−Fulcher−Tammann (VFT) approximation[58] ($\eta = \eta_0 \exp[DT_0/(T - T_0)]$), and the best-fit parameters are listed in Table 4. It is reasonable that the T_0 values, corresponding to the ideal glass-transition temperatures, were lower than the T_g values observed by the DSC measurements. The D values, indicating the degree of deviation from Arrhenius behavior,[59] increased with increasing alkyl chain length. A similar tendency of VFT parameters has been reported for the electrical conductivities of 1-alkyl-3-methylimidazolium tetrafluoroborate.[60] The small values of D for [**1**][TFSA] and [**2**][TFSA], which are comparable to [C_4mim][TFSA] and [butylferrocenium][TFSA] (Table 4), indicate that they are fragile liquids,[61,62] whereas the larger values for [**5**][TFSA] and [**6**][TFSA] indicate less fragility.

Table 5. Redox Potentials from Cyclic Voltammetry of [**1**][PF_6], [**9**][PF_6], *N*-Ferrocenylimidazole, and 4-Ferrocenyltriazole in 0.1 M *n*-Bu_4NClO_4−MeCN (in *V* vs $FeCp_2/FeCp_2^+$)

	$Fc^{0/+}$			[Azole group]$^{+/0}$
compd	E_p^c	E_p^a	$E_{1/2}$	E_p^c
[**1**][PF_6]	0.27	0.34	0.31	−1.56
[**9**][PF_6]	0.32	0.39	0.36	−1.26
N-ferrocenylimidazole	0.10	0.17	0.14	
4-ferrocenyltriazole [a]	0.17	0.24	0.21	
4-ferrocenyltetrazole [a]	0.24	0.30	0.27	

[a] See ref 63.

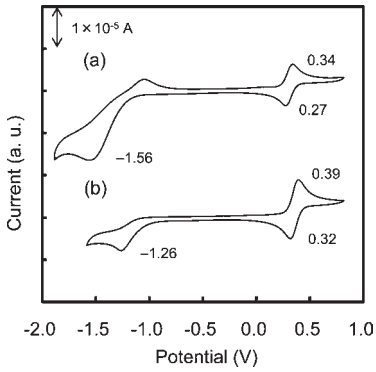

Figure 4. Cyclic voltammograms of (a) [**1**][PF_6] and (b) [**9**][PF_6] in acetonitrile (vs $FeCp_2/FeCp_2^+$).

Redox Properties. The redox properties of [**1**][PF_6], [**9**][PF_6], *N*-ferrocenylimidazole, and 4-ferrocenyltriazole in acetonitrile solution were investigated using cyclic voltammetry. Table 5 lists the measured redox potentials of the ferrocenyl and azolium moieties. Figure 4 shows the cyclic voltammograms of [**1**][PF_6] and [**9**][PF_6]. Reversible redox

(54) Zhou, Z. -B.; Matsumoto, H. *Electrochem. Commun.* **2007**, *9*, 1017–1022.
(55) Bradley, A. E.; Hardacre, C.; Holbrey, J. D.; Johnston, S.; McMath, S. E. J.; Nieuwenhuyzen, M. *Chem. Mater.* **2002**, *14*, 629–635.
(56) Paul, A.; Samanta, A. *J. Phys. Chem. B* **2008**, *112*, 16626–16632.
(57) Inagaki, T.; Mochida, T., in preparation.
(58) Fulcher, G. S. *J. Am. Ceram. Soc.* **1925**, *8*, 339–355.
(59) Harris, K. R.; Kanakubo, M.; Woolf, L. A. *J. Chem. Eng. Data* **2007**, *52*, 2425–2430.
(60) Leys, J.; Wübbenhorst, M.; Menon, C. P.; Rajesh, R.; Thoen, J.; Glorieux, C.; Nockemann, P.; Thijs, B.; Binnemans, K.; Longuemart, S. *J. Chem. Phys.* **2008**, *128*, 064509.
(61) Angell, C. A. *J. Non-Cryst. Solids* **1985**, *73*, 1–17.
(62) Xu, W.; Cooper, E. I.; Angell, C. A. *J. Phys. Chem. B* **2003**, *107*, 6170–6178.

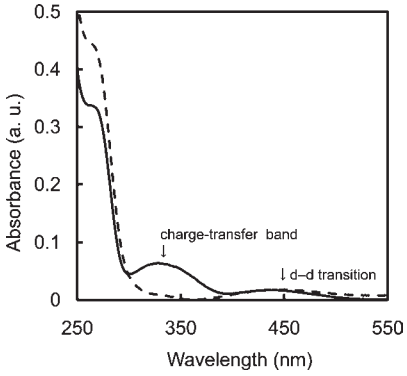

Figure 5. UV−vis absorption spectra of [**1**][PF_6] (solid line) and *N*-ferrocenylimidazole (dashed line) in dichloromethane.

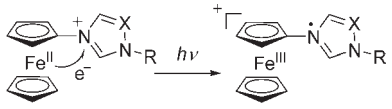

Figure 6. Schematic illustration of photoinduced charge-transfer in ferrocenylazolium cations (X = CH or N).

waves for the ferrocenyl moieties were observed at $E_{1/2}$ = 0.31 and 0.36 V (vs $FeCp_2/FeCp_2^+$), respectively, which are higher than those for *N*-ferrocenylimidazole and 4-ferrocenyltriazole[63] by ca. 0.16 V. This result is consistent with the formation of azolium cations. For [**1**][PF_6] and [**9**][PF_6], irreversible redox waves for the azole moieties were observed at $E_p^c = -1.56$ and −1.26 V, respectively. The redox potential of [**1**][PF_6] and *N*-ferrocenylimidazole are lower than that of [**9**][PF_6] and 4-ferrocenyltriazole by ca. 0.06 V, which reflects the weaker electron-withdrawing effect of imidazole.

UV−Vis Absorption Spectra. The UV−vis absorption spectra of [**1**][PF_6] and *N*-ferrocenylimidazole in dichloromethane solutions are shown in Figure 5. The broad absorption band at λ_{max} = 328 nm in [**1**][PF_6], which is absent in *N*-ferrocenylimidazole, is assignable to a CT band from the ferrocenyl moiety to the imidazolium moiety (Figure 6). The absorption bands at around 270 and 442 nm are $\pi-\pi^*$[64] and d−d transitions,[65] respectively, with the latter probably mixed with d−π^* transitions. No absorption bands were observed in the longer wavelength region up to 1800 nm. The spectrum of [**1**][TFSA] in dichloromethane was identical to that of [**1**][PF_6]. The CT band in [**9**][PF_6] was observed at a longer wavelength (λ_{max} = 334 nm), which corresponds to the stronger electron accepting ability of the azole moieties, as seen in the electrochemical analysis. CT bands of donor−acceptor molecules are often observed at longer wavelengths. A ferrocene−viologen compound, for example, exhibits CT bands at around 600 nm.[66] In the present salts, however, the absorption bands were observed at higher energies because of the weaker electron affinity of the imidazolium moiety.

Spectral data for [**1**][PF_6] in various solvents are summarized in Table 6. CT bands in tetrahydrofuran, acetonitrile, and methanol, which are solvents with higher donor numbers, exhibited a blue-shift by about 10 nm compared with the spectra in dichloromethane, whereas the $\pi-\pi^*$ transitions were solvent-independent. CT bands often exhibit a large solvent effect,[67] but the effect in the present salts was smaller than typically seen due to the large excitation energy, which made the solvent effect relatively small. In dichloromethane solution, the CT band of [**1**][TFSA] appeared at about the same position as [**1**][PF_6] (λ_{max} = 332 nm), whereas in the neat liquid, the band was observed at λ_{max} = 320 nm, as was seen in the methanol solution. Because the solvent polarity of the salt is comparable to that of methanol, this result is probably due to the solvent effect of the ionic liquid itself.

Analysis of Photoinduced Electron Transfer. Photoinduced intramolecular electron-transfer in a molecular system is often analyzed based on the Marcus−Hush model using $h\nu_{max} = \Delta G + \lambda$, where ΔG, λ, and $h\nu_{max}$ are the free energy difference, reorientation energy, and energy of the charge-transfer absorption band, respectively.[32,68] This model was applied to the present salts. The delocalization coefficient α was estimated based on $\alpha^2 = 4.24 \times 10^{-4}\ \varepsilon_{max}\Delta\tilde{\nu}_{1/2}/(h\nu_{max}r^2)$, where r, ν_{max}, $\Delta\tilde{\nu}_{1/2}$, and ε_{max} are the distance between D and A centers, the wavelength of maximum absorption for the CT band, the absorption bandwidth at half-height, and the molar absorbance coefficient, respectively. The distances between Fe and N_{-Fc} determined by X-ray structure analyses of [**1**][PF_6] and [**9**][I] (vide infra) were tentatively used as the values of r, 3.094 and 3.126 Å, respectively. The oscillator strength f of the CT band was calculated as $f = 4.6 \times 10^{-9}\ \varepsilon_{max}\Delta\tilde{\nu}_{1/2}$,[69] and the effective electronic coupling V_{D-A} (donor−acceptor coupling term) was estimated by the Hush formula, or $V_{D-A} = \alpha\tilde{\nu}_{max}$.[68] ΔG is approximated as the difference between the redox potentials of the ferrocenyl moiety and the azolium moiety (ΔE). Table 7 shows the parameters obtained for **1** and **9** by using these fomulae. The differences in their CT energies consistently reflect the electron-withdrawing effect of the azolium moieties. The differences, however, are smaller than the redox potential differences, which is possibly due to the differences in the reorientation energies λ and their electronic structures. As expected, these salts were confirmed to be unsymmetrical class II mixed-valence complexes,[70] whose α^2 values are in the range of 0−0.5. Values for V_{D-A} thus obtained are much larger than those in related systems such as aza-substituted ferrocenes[33] and diferrocenylpolyenes,[71] whose V_{D-A} are about 500−600 cm^{-1}. This result suggests a large D−A interaction in the present salts, resulting predominantly from the large excitation energy. The values of α are also larger than those in the related systems.

Crystal Structures. To obtain structural information, we determined crystal structures for [**1**][PF_6], [**4**][TFSA], and [**9**][I]. The structures of the cations in these salts are

(63) Mochida, T.; Shimizu, H.; Suzuki, S.; Akasaka, T. *J. Organomet. Chem.* **2006**, *691*, 4882–4889.
(64) Camire, N.; Mueller-Westerhoff, U. T.; Geiger, W. E. *J. Onganomet. Chem.* **2001**, *637−639*, 823–826.
(65) Rosenblum, M.; Santer, J. O.; Howells, W. G. *J. Am. Chem. Soc.* **1963**, *85*, 1450–1458.
(66) Nishikitani, Y.; Uchida, S.; Asano, T.; Minami, M.; Oshima, S.; Ikai, K.; Kubo, T. *J. Phys. Chem. C* **2008**, *112*, 4372–4377.
(67) Reichardt, C. *Chem. Rev.* **1994**, *94*, 2319–2358.
(68) Hush, N. S. *Coord. Chem. Rev.* **1985**, *64*, 135–137.
(69) Zhu, Y.; Wolf, M. O. *J. Am. Chem. Soc.* **2000**, *122*, 10121–10125.
(70) Robin, M. B.; Day, P. *Adv. Inorg. Chem. Radiochem.* **1967**, *10*, 247–422.
(71) Ribou, A. -C.; Launay, J. -P.; Sachtleben, M. L.; Li, H.; C. W. Spangler, C. W. *Inorg. Chem.* **1996**, *35*, 3735–3740.

Table 6. Spectral Data for [**1**][TFSA], [**1**][PF_6], and [**9**][PF_6]

compd	solvent	$\pi-\pi^*$ transition (nm)	CT band (nm)	ε_{CT} (L mmol^{-1} cm^{-1})	d−d transition (nm)	ε_{d-d}(L mmol^{-1} cm^{-1})
[**1**][TFSA]	CH_2Cl_2	268[a]	332	1.052	438	0.403
	(neat)	264	320		440	
[**1**][PF_6]	CH_3OH	268	320	1.078	436	0.296
	CH_3CN	268	318[a]	0.990	438	0.260
	CH_2Cl_2	270[a]	328	0.929	442	0.246
	THF	268	318	0.945	436	0.219
[**9**][PF_6]	CH_2Cl_2	266	334	0.918	434	0.312

[a] Shoulder.

Table 7. Parameters Related to Photoinduced Intramolecular Electron Transfer (See Text)

compd	ΔE_{Fc-Az} (V)	ΔG (cm^{-1})	$\tilde{\nu}_{max}$ (cm^{-1})	λ (cm^{-1})	ε_{max}(M^{-1} cm^{-1})	$\Delta\tilde{\nu}_{1/2}$ (cm^{-1})	$f \times 10^3$	V_{D-A} (cm^{-1})	α
[**1**][PF_6]	1.834	14792	30488	15696	929	69444	297	9338	0.31
[**9**][PF_6]	1.582	12760	30120	17361	918	56818	240	8260	0.27

shown in Figure S4 in the Supporting Information. In these molecules, Fe−C(Cp) bond lengths were typical of monosubstituted ferrocenes,[72] and the Fe−C_A(Cp) distance, where C_A is the carbon to which the azole ring is attached, were the shortest among them. The Cp rings of the ferrocenyl moieties exhibited an eclipsed conformation. The torsion angles between the azole ring and the adjacent Cp ring varied between 24.1(2) and 37.10(9), suggesting that the torsion angle is susceptible to intermolecular packing forces. The butyl substituent in **4** exhibited an all-trans conformation. There were no intermolecular contacts between the alkyl groups. In all of the structures, the ferrocenyl moieties of the neighboring molecules were orthogonal with each other, and no direct intermolecular $\pi-\pi$ contacts were found.

The packing diagram of [**4**][TFSA] is shown in Figure 7a. The anions and cations were alternately arranged in the crystal. The anion adopted a *trans* configuration. This salt exhibited short hydrogen-bond-like CH···O intermolecular contacts of 2.351(1) Å between the imidazolium hydrogen at the C5 position and an oxygen atom of the anion, which is notably shorter than the sum of the van der Waals (vdW) radii (2.72 Å) by 0.37 Å. There was also another short H(Cp)···O_{anion} contact of 2.333(1) Å. These short contacts formed a one-dimensional chain network along the *a* axis (Figure 7a, dashed lines). There were other contacts between the anion and imidazolium hydrogens of adjacent cations (CH···O = 2.595(1) Å, 2.554(1) Å, 2.563(1) Å). Hydrogen-bond-like CH···X interactions[73] between the hydrogen at the C2 position of the cation and an electronegative atom of the anion, which is associated with the high acidity of the hydrogen,[74] are often seen in the crystal structures of imidazolium salts. For example, short contacts such as CH···F = 2.49(2) Å in [Emim][PF_6][75] and CH···I = 2.928 Å in [Emim][I][76] are found, which are shorter than the vdW distances by 0.18 Å and 0.252 Å, respectively. In [**4**][TFSA], however, the contact involving the C2 hydrogen (2.595(1) Å) was longer than the other contacts.

Packing diagrams for [**1**][PF_6] and [**9**][I] are shown in diagrams b and c in Figure 7, respectively. In terms of intermolecular interaction, both salts formed layerlike structures in which the azolium moiety and the anion constructed an ionic 2D network structure via intermolecular contacts shorter than the vdW distances. In [**1**][PF_6], CH···F contacts (2.491(1) Å) involving the C2 hydrogen and C_{azole}···F contacts formed the ionic layer in the *ab* plane, to which ferrocenyl moieties are attached as pendants to form neutral layers. In [**9**][I], the iodide ion was placed above the azole ring of the nearest cation and contacted by two azole hydrogens of neighboring cations (CH···I = 2.9933(9) Å, 3.0054(9) Å) (see Figure S5 in the Supporting Information). There are similar CH···X interactions in the crystals of [$C_n$mim][I] and related halides,[77] but no network structure is formed in [Emim][I], which consists of an ion-pair joined by two CH···I interactions.[76] Dialkylimidazolium salts such as [Mmim][TFSA][17] and those with long alkyl chains[55] exhibit layerlike structures. We expected that the CH···X interactions might become weaker because of a decrease in the acidity of the hydrogens resulting from the presence of the electron-releasing ferrocenyl substituent, but no such tendency could be detected from these structural investigations.

Conclusion

A series of imidazolium-based ILs with a ferrocenyl substituent have been prepared. These salts exhibited higher melting points and higher viscosities as compared with usual dialkylimidazolium salts. The compounds are redox active salts with ferrocene as the donor moiety and the azolium cation as the acceptor moiety. Corresponding charge-transfer absorption bands were observed and interpreted using the Marcus−Hush model, and the interaction between the donor−acceptor was found to be strong. These electrochemical and photophysical properties reflect the stronger electron withdrawing property of triazole compared to imidazole. Crystal structure determinations revealed that these salts exhibited network structures via CH···X contacts (X = O, F, and I). The imidazolium salts may be useful for the investigation of photoinduced electron transfer in the neat

(72) Lousada, C. M.; Pinto, S. S.; Lopes, J. N. C.; Piedade, M. F. M.; Diogo, H. P.; Piedade, M. E. M. *J. Phys. Chem. A* **2008**, *112*, 2977–2987.
(73) Desiraju, G. R.; Steiner, T.; *The Weak Hydrogen Bond in Structural Chemistry and Biology; IUCR Monographs on Crystallography 9*; Oxford University Press: Oxford, U.K., 1999.
(74) Fuller, J.; Carlin, R. T.; Long, H. C. D.; Haworth, D. *J. Chem. Soc., Chem. Commun.* **1994**, 299–300.
(75) Reichert, W. M.; Holbey, J. D.; Swatloski, R. P.; Gutowski, K. E.; Visser, A. E.; Nieuwenhuyzen, M.; Seddon, K. R.; Rogers, R. D. *Cryst. Growth Des.* **2007**, *7*, 1106–1114.
(76) Abdul-Sada, A. K.; Greenway, A. M.; Hitchcock, P. B.; Mohammed, T. J.; Seddon, K. R.; Zora, J. A. *J. Chem. Soc., Chem. Commun.* **1986**, 1753–1754.
(77) Elaiwi, A.; Hitchcock, P. B.; Seddon, K. R.; Srinivasan, N.; Tan, Y. -M.; Welton, T.; Zora, J. A. *J. Chem. Soc., Dalton Trans.* **1995**, 3467–3472.

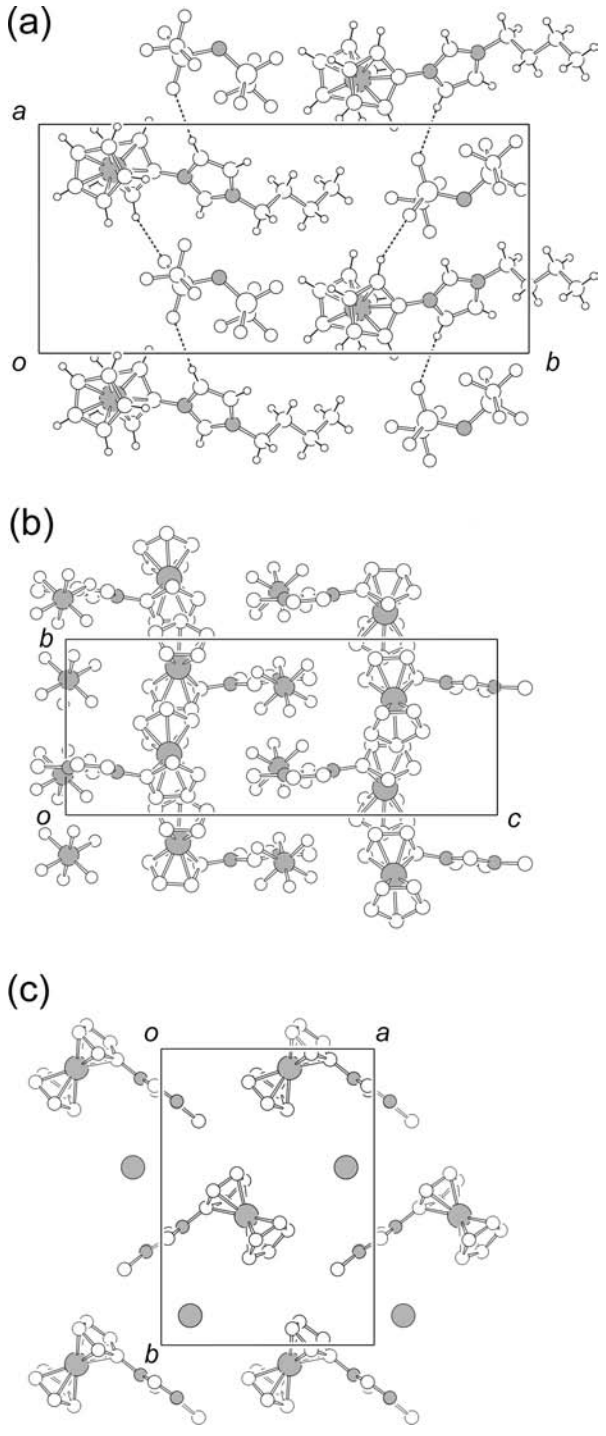

Figure 7. Packing diagrams of (a) [**4**][TFSA], (b) [**1**][PF_6], and (c) [**9**][I]. Dashed lines represent intermolecular short CH···O contacts. Hydrogen atoms have been omitted for clarity in (b) and (c).

liquid state and also for applications such as redox active liquids.

Experimental Section

General. *N*-Ferrocenylimidazole and 4-ferrocenyltriazole were prepared according to literature methods.[78,63] Other solvents and reagents were commercially available. Modification of the procedure for synthesis of *N*-ferrocenylimidazole, including the use of twice the amount of solvent and a higher reaction temperature (100 °C) for a longer time (2 days) followed by crystallization via slow evaporation of an ether solution led to an increase in the yield from 31%[78] to 62%. ^{1}H NMR spectra were recorded on a JEOL JNM-ECL-400 spectrometer. Elemental analyses were performed using a Yanaco CHN coder MT-5. Viscosities were measured with a Toki Sangyo TV-22 viscometer using a 3° × R7.7 cone rotor. DSC measurements were performed using a TA Instrument Q100 differential scanning calorimeter. UV−vis absorption spectra were recorded on a JASCO V-570 UV/VIS/NIR spectrophotometer. UV−vis absorption spectra of neat ILs were measured by using thin quartz plates. Cyclic voltammograms were recorded with an ALS/chi electrochemical analyzer model 600A. Redox potentials were measured at a scan rate of 0.1 V s^{-1} in acetonitrile containing 0.1 mol dm^{-3} *n*-Bu_4NClO_4 as the supporting electrolyte. An Ag/Ag^+ reference electrode and a platinum working electrode were used, and the potentials were referenced to a $FeCp_2/FeCp_2^+$ couple.

X-ray Structure Determinations. Single crystals of [**4**][TFSA] suitable for X-ray analysis were obtained by the diffusion method (*n*-hexane/dichloromethane). Other crystals were obtained by slow cooling of saturated solutions: [**1**][PF_6] from ethanol, and [**9**][I] from acetonitrile. X-ray diffraction data were collected on Bruker CCD diffractometers (APEX II ultra and Smart 1000) using MoKα radiation (λ = 0.71073 Å). The data were corrected for absorption by using the SADABS program.[79] The structures were solved by direct methods (SHELXS 97[80]) and expanded using Fourier techniques. The non-hydrogen atoms were refined anisotropically. Crystallographic parameters are listed in Table 8. The ORTEP-3 program was used for molecular graphics.[81] CCDC-775317 (for [**1**][PF_6]), -680034 (for [**9**][I]), and -775316 (for [**4**][TFSA]) contain the supplementary crystallographic data for this paper. These data can be obtained free of charge from The Cambridge Crystallographic Data Centre via www.ccdc.cam.ac.uk/data_request/cif.

1-Ferrocenyl-3-methylimidazolium Salts ([1][X]; X = I, TFSA, PF_6). (a) 1-Ferrocenyl-3-methylimidazolium iodide ([**1**][I]). Under a nitrogen atmosphere, *N*-ferrocenylimidazole (96.0 mg, 0.381 mmol) was dissolved in iodomethane (4 mL) and the solution stirred for 3 h at room temperature. The precipitated product was collected by filtration, washed with ether, and vacuum-dried to provide an orange powder in 97.4% yield (146 mg). The product was recrystallized three times from ethanol. Mp 194 °C. ^{1}H NMR (400 MHz, DMSO-d_6, ppm) δ = 3.88 (s, 3H), 4.31 (s, 5H), 4.41 (t, 2H, J = 2.0 Hz), 5.02 (t, 2H, J = 2.0 Hz), 7.85 (s, 1H), 8.14 (s, 1H), 9.55 (s, 1H). Anal. Found: C, 42.79; H, 3.81; N, 6.68%. Calcd for $C_{14}H_{15}F_6FeN_2I$: C, 42.67; H, 3.84; N, 7.11%. (b) 1-Ferrocenyl-3-methylimidazolium TFSA ([**1**][TFSA]). An aqueous solution of LiTFSA (90.2 mg, 0.314 mmol) was added dropwise to an aqueous solution of [**1**][I] (79.3 mg, 0.201 mmol), and the solution was stirred for a few hours at room temperature. A red-brown oil separated from the water phase. The mixture was extracted with dichloromethane and the organic layer washed with water and dried over magnesium sulfate. The solvent was then evaporated under reduced pressure and the product vacuum-dried at 80 °C for 24 h to give a red-brown oil in 99.0% yield (109 mg). The salt crystallized when allowed to stand at room temperature after being cooled once to −50 °C. Mp 34.6 °C (DSC). ^{1}H NMR (DMSO-d_6, ppm) δ = 3.88 (s, 3H), 4.31 (s, 5H), 4.40 (t, 2H, J = 1.8 Hz), 5.02 (t, 2H, J = 1.8 Hz), 7.85 (s, 1H), 8.13 (s, 1H), 9.54 (s, 1H). Anal. Found: C, 35.21; H, 2.97; N, 7.59%. Calcd for $C_{16}H_{15}F_6FeN_3O_4S_2$: C, 35.11; H, 2.76; N, 7.68%. (c) 1-Ferrocenyl-3-methylimidazolium hexafluorophosphate ([**1**][PF_6]). [**1**][I] (83.0 mg, 0.211 mmol) was dissolved in a small amount

(78) Özçubukçu, S.; Schmitt, E.; Leifert, A.; Bolm, C. *Synthesis* **2007**, *3*, 0389–0392.

(79) Sheldrick, G. M. *SADABS; Program for Semi-empirical Absorption Correction*; University of Göttingen: Göttingen, Germany, 1996.

(80) Sheldrick, G. M. *Program for the Solution for Crystal Structures*; University of Göttingen: Göttingen, Germany, 1997.

(81) Farrugia, L. J. *J. Appl. Crystallogr.* **1997**, *30*, 565.

Table 8. Crystallographic Parameters

	[**4**][TFSA]	[**1**][PF_6]	[**9**][I]
empirical formula	$C_{19}H_{21}F_6FeN_3O_4S_2$	$C_{14}H_{15}F_6FeN_2P$	$C_{13}H_{14}FeIN_3$
fw (g mol^{-1})	589.36	412.10	395.02
cryst syst	monoclinic	monoclinic	monoclinic
space group	$P2_1/c$ (No. 14)	$P2_1/n$ (No. 14)	$P2_1/c$ (No. 14)
a (Å)	9.7368(5)	10.0122(14)	10.163(4)
b (Å)	20.6111(10)	7.8662(11)	13.981(5)
c (Å)	11.8747(6)	19.688(3)	9.696(3)
β (deg)	97.649(1)	101.454(2)	98.553(5)
volume (Å^3)	2361.9(2)	1519.7(4)	1362.4(8)
Z	4	4	4
d_{calcd} (g cm^{-3})	1.657	1.801	1.926
T (K)	100	100	100
μ (mm^{-1})	0.895	1.163	3.358
no. of reflns collected	13377	7019	15227
no. of independent reflns	4841 (R_{int} = 1.5%)	2675 (R_{int} = 1.5%)	5587 (R_{int} = 4.0%)
parameters	317	218	164
$R_1{}^a$, $wR_2{}^b$ ($I > 2\sigma(I)$)	0.0238, 0.0622	0.0210, 0.0526	0.0424, 0.1063
$R_1{}^a$, $wR_2{}^b$ (all data)	0.0265, 0.0642	0.0223, 0.0536	0.0519, 0.1127
goodness-of-fit on F^2	1.030	1.068	1.082
diffractometer	Smart 1000	APEX II ultra	APEX II ultra

[a] $R_1 = \Sigma||F_o|-|F_c||/\Sigma|F_o|$. [b] $wR_2 = [\Sigma w(F_o^2 - F_c^2)^2/\Sigma w(F_o^2)^2]^{1/2}$.

of water. To this solution was added dropwise an aqueous solution of $NaPF_6$ (62.0 mg, 0.369 mmol) followed by stirring for a few hours. A yellow powder precipitated and was collected by filtration and vacuum-dried. The product was recrystallized from ethanol as yellow needles in 76.4% yield (66.3 mg). Mp 147.2 °C (DSC). ^{1}H NMR (DMSO-d_6, ppm) δ = 3.88 (s, 3H), 4.31 (s, 5H), 4.41 (t, 2H, J = 2.0 Hz), 5.02 (t, 2H, J = 1.9 Hz), 7.85 (s, 1H), 8.13 (s, 1H), 9.55 (s, 1H). Anal. Found: C, 40.83; H, 3.64; N, 6.72%. Calcd for $C_{14}H_{15}F_6FeN_2P$: C, 40.80; H, 3.67; N, 6.80%.

1-Ferrocenyl-3-ethylimidazolium Salts ([2][X], X = TFSA, PF_6). (a) 1-Ferrocenyl-3-ethylimidazolium TFSA ([**2**][TFSA]). [**2**][I] was prepared as described for [**1**][I]. The reaction was carried out at 45 °C for 4 h to give a yellow powder in 92.4% yield. ^{1}H NMR (DMSO-d_6, ppm) δ = 1.49 (t, 3H, J = 7.2 Hz), 4.23 (q, 2H, J = 7.2 Hz), 4.31 (s, 5H), 4.41 (t, 2H, J = 1.8 Hz), 5.03 (t, 2H, J = 2.0 Hz), 7.97 (s, 1H), 8.18 (s, 1H), 9.59 (s, 1H). The TFSA salt was prepared as described for [**1**][TFSA], except that the product was washed with hexane several times under sonification, extracted with dichloromethane, purified through a short plug of alumina, and then vacuum-dried at 80 °C to give a red-brown oil in 86.5% yield. Crystallization occurred when the oil was placed in a plastic bottle and stored in a freezer. Mp 37.6 °C (DSC). ^{1}H NMR (DMSO-d_6, ppm) δ = 1.49 (t, 3H, J = 7.4 Hz), 4.22 (q, 2H, J = 7.3 Hz), 4.31 (s, 5H), 4.41 (t, 2H, J = 1.8 Hz), 5.03 (t, 2H, J = 1.8 Hz), 7.97 (s, 1H), 8.17 (s, 1H), 9.58 (s, 1H). Anal. Found: C, 36.26; H, 3.04; N, 7.49%. Calcd for $C_{17}H_{17}F_6FeN_3O_4S_2$: C, 36.38; H, 3.05; N, 7.49%. (b) 1-Ferrocenyl-3-ethylimidazolium hexafluorophosphate ([**2**][PF_6]). This salt was prepared as described for [**1**][PF_6] and recrystallized from ethanol to give a yellow powder in 65.2% yield. Mp 123.2 °C (DSC). ^{1}H NMR (DMSO-d_6, ppm) δ = 1.49 (t, 3H, J = 7.4 Hz), 4.22 (q, 2H, J = 7.3 Hz), 4.31 (s, 5H), 4.41 (t, 2H, J = 2.0 Hz), 5.03 (t, 2H, J = 2.0 Hz), 7.96 (s, 1H), 8.17 (s, 1H), 9.58 (s, 1H). Anal. Found: C, 42.13; H, 4.32; N, 6.57%. Calcd for $C_{15}H_{17}F_6FeN_2P$: C, 42.28; H, 4.02; N, 6.57%.

1-Ferrocenyl-3-butylimidazolium Salts ([4][X]; X = TFSA, PF_6). (a) 1-Ferrocenyl-3-butylimidazolium TFSA ([**4**][TFSA]). [**4**][I] was prepared by using toluene as a solvent: iodo-*n*-butane (2.67 g, 14.5 mmol) was added dropwise to a solution of *N*-ferrocenylimidazole (254 mg, 1.01 mmol) in toluene (50 mL) with stirring. This solution was refluxed for 20 h under a nitrogen atmosphere. After cooling the solution, a dark-brownish powder precipitated, which dissolved after addition of water and toluene followed by warming. The muddy yellow aqueous layer containing the iodide was separated and used for the next step. ^{1}H NMR (DMSO-d_6, ppm) δ = 0.93 (t, 3H, J = 7.6 Hz), 1.31 (se, 2H, J = 7.2 Hz), 1.85 (q, 2H, J = 7.6 Hz), 4.19 (t, 2H, J = 7.2 Hz), 4.30 (s, 5H), 4.41 (t, 3H, J = 7.2 Hz), 5.04 (t, 2H, J = 2.0 Hz), 7.97 (s, 1H), 8.18 (s, 1H), 9.62 (s, 1H). The TFSA salt was prepared as described for [**2**][TFSA] to give a red-brown oil in 77.2% yield (459 mg). Crystallization occurred when the oil was scratched in a bottle to give red-brown crystals. Mp 50.1 °C (DSC). ^{1}H NMR (DMSO-d_6, ppm) δ = 0.93 (t, 3H, J = 7.4 Hz), 1.31 (m, 2H), 1.85 (qu, 2H, J = 7.5 Hz), 4.19 (t, 2H, J = 7.4 Hz), 4.30 (s, 5H), 4.41 (d, 2H, J = 2.0 Hz), 5.04 (t, 2H, J = 2.0 Hz), 7.96 (s, 1H), 8.18 (s, 1H), 9.61 (s, 1H). Anal. Found: C, 38.84; H, 3.57; N, 6.85%. Calcd for $C_{19}H_{21}F_6FeN_3O_4S_2$: C, 38.72; H, 3.59; N, 7.13%. (b) 1-Ferrocenyl-3-butylimidazolium hexafluorophosphate ([**4**][PF_6]). This salt was prepared as described for [**1**][PF_6], except that the product was extracted with dichloromethane, washed with water, dried over magnesium sulfate, washed with hexane for several times under sonification, extracted with dichloromethane, purified through a short plug of alumina, and vacuum-dried at 80 °C to give a yellow powder in 76.1% yield. Crystallization occurred when the oil was stored in a freezer. Mp 87.7 °C (DSC). ^{1}H NMR (DMSO-d_6, ppm) δ = 0.93 (t, 3H, J = 7.4 Hz), 1.31 (q, 2H, J = 7.6 Hz), 1.85 (qu, 2H, J = 7.5 Hz), 4.19 (t, 2H, J = 7.2 Hz), 4.30 (s, 5H), 4.41 (t, 2H, J = 2.0 Hz), 5.04 (t, 2H, J = 1.8 Hz), 7.96 (s, 1H), 8.18 (s, 1H), 9.62 (s, 1H). Anal. Found: C, 45.10; H, 4.87; N, 6.21%. Calcd for $C_{17}H_{21}F_6FeN_2P$: C, 44.96; H, 4.66; N, 6.17%.

1-Ferrocenyl-3-dodecylimidazolium Salts ([7][X]; X = TFSA, PF_6). (a) 1-Ferrocenyl-3-dodecylimidazolium TFSA ([**7**][TFSA]). [**7**][I] was prepared as described for [**4**][I]. After evaporation of the solvent, methanol was added, and the mixture washed with *n*-hexane. The methanol layer was separated and used for the preparation of the TFSA salt. TFSA salt was prepared as described for [**1**][TFSA]. The product was extracted with dichloromethane, the organic layer washed with water, and the solvent evaporated. The residue was dissolved in methanol, washed with hexane, and the solvent evaporated. The residue was extracted with dichloromethane, purified through a short plug of alumina, and vacuum-dried at 80 °C to give a red-brown oil in 55.7% yield. ^{1}H NMR (DMSO-d_6, ppm) δ = 0.85 (t, 3H, J = 6.8 Hz), 1.23 (m, 18H), 1.87 (m, 2H), 4.18 (t, 2H, J = 7.2 Hz), 4.29 (s, 5H), 4.41 (t, 2H, J = 1.9 Hz), 5.04 (t, 2H, J = 2.1 Hz), 7.96 (s, 1H), 8.18 (s, 1H), 9.62 (s, 1H). Anal. Found: C, 46.81; H, 5.70; N, 5.90%. Calcd for $C_{27}H_{37}F_6FeN_3O_4S_2$: C, 46.22; H, 5.32; N, 5.99%. (b) 1-Ferrocenyl-3-dodecylimidazolium hexafluorophosphate ([**7**][PF_6]). This salt was prepared as described for [**7**][TFSA], except that $NaPF_6$ was used instead of LiTFSA, and the product was vacuum-dried at room temperature. The product was purified by slow diffusion of

n-hexane into a dichloromethane solution to give a yellow powder in 46.4% yield. Mp 94.2 °C (DSC). ^{1}H NMR (DMSO-d_6, ppm) δ = 0.85 (t, 3H, J = 6.8 Hz), 1.23 (m, 18H), 1.86 (m, 2H), 4.18 (t, 2H, J = 7.4 Hz), 4.29 (s, 5H), 4.41 (t, 2H, J = 2.0 Hz), 5.04 (t, 2H, J = 2.0 Hz), 7.96 (s, 1H), 8.18 (s, 1H), 9.62 (s, 1H). Anal. Found: C, 52.98; H, 6.50; N, 4.93%. Calcd for $C_{25}H_{37}F_6FeN_2P$: C, 53.01; H, 6.58; N, 4.95%.

1-Ferrocenyl-4-methyltriazolium Salts ([9][X]; X = I, PF_6). (a) 1-Ferrocenyl-4-methyltriazolium iodide ([**9**][I]). A mixture of 4-ferrocenyltriazole (37.1 mg, 0.147 mmol) and an excess of iodomethane (4 mL) was refluxed under a nitrogen atmosphere for 3 h. The precipitated product was collected by filtration, washed with ether, and dried under a vacuum to give yellow powders in 72.7% yield. ^{1}H NMR (DMSO-d_6, ppm) δ = 4.09 (s, 3H), 4.37 (s, 5H), 4.46 (t, 2H, J = 2.0 Hz), 5.02 (t, 2H, J = 2.0 Hz), 9.59 (s, 1H), 10.52 (s, 1H). Anal. Found: C, 39.69; H, 3.58; N, 10.01%. Calcd for $C_{13}H_{14}FeN_3I$: C, 39.53; H, 3.57; N, 10.64%. (b) 1-Ferrocenyl-4-methyltriazolium hexafluorophosphate ([**9**][PF_6]). This salt was prepared as described for [**1**][PF_6] to give a yellow powder in 83.7% yield. Mp 198 °C (dec.). ^{1}H NMR (DMSO-d_6, ppm) δ = 4.08 (s, 3H), 4.36 (s, 5H), 4.44 (t, 2H, J = 1.8 Hz), 5.01 (t, 2H, J = 2.0 Hz), 9.57 (s, 1H), 10.49 (s, 1H). Anal. Found: C, 38.07; H, 3.63; N, 10.15%. Calcd for $C_{13}H_{14}F_6FeN_3P$: C, 37.80; H, 3.42; N, 10.17%.

Other salts ([**3**][TFSA], [**5**][TFSA], [**6**][TFSA], [**6**][PF_6], [**8**][TFSA], [**8**][PF_6]) were prepared similarly (see the Supporting Information).

Acknowledgment. This work was financially supported by a Grant-in-Aid for Scientific Research (21350077) from Japan Society for the Promotion of Science (JSPS) and the "High-Tech Research Center" Project in Toho University (2005−2009) from Ministry of Education, Culture, Sports, Science and Technology (MEXT). We thank T. Inagaki (Kobe University) for his help with experiments, Y. Furuie (Kobe University) for elemental analysis, and M. Nakama (WarpStream Ltd., Tokyo) for providing Web-database systems. We thank Dr. K. Yoza (Bruker ASX Japan) for the structure determination of [**9**][I].

Supporting Information Available: A schematic Gibbs free energy diagram for [**8**][PF_6] (Figure S1); DSC thermograms of [**8**][PF_6] (Figure S2); temperature dependence of the viscosities (Figure S3); molecular structures of the cations in [**1**][PF_6], [**4**][TFSA], and [**9**][I] (Figure S4); schematic illustration of the cation−anion contacts in [**9**][I] (Figure S5); experimental details of synthesis and characterization data for [**3**][TFSA], [**5**][TFSA], [**6**][X], and [**8**][X] (X = TFSA, PF_6) (PDF); and crystallographic information files (CIFs) for [**1**][PF_6], [**9**][I], and [**4**][TFSA]. This material is available free of charge via the Internet at http://pubs.acs.org.